ELSEVIER

Catena 46 (2001) 125–139

CATENA

www.elsevier.com/locate/catena

Evolution of soil surface roughness and flowpath connectivity in overland flow experiments

F. Darboux [a,b,*], Ph. Davy [a,1], C. Gascuel-Odoux [b,2], C. Huang [c,3]

[a] *Géosciences Rennes, UPR 4661, Campus de Beaulieu, University Rennes 1, F-35042 Rennes Cedex, France*
[b] *Unité Sol-Agronomie de Rennes-Quimper, INRA, 65, rue de St-Brieuc, F-35042 Rennes Cedex, France*
[c] *National Soil Erosion Research Laboratory, USDA-ARS, Purdue University, Building SOIL, West Lafayette, IN 47907-1196, USA*

Abstract

During rainfall events, surface roughness affects runoff generation by providing water surface storage in the depressions and altering the flow direction on the surface. The process of runoff initiation, or triggering, involves the gradual filling of individual depressions and the connection of those overflowing depressions toward the outflow boundary. Although studies have been conducted to relate surface roughness to total depression storage, little work has been done in quantifying the roughness effects on runoff initiation. This study examines the role of surface roughness on overland flow triggering in interrill areas. Laboratory experiments were conducted on a 2.4-m × 2.4-m soil box exposed to a sequence of four rainfall events with treatments including two levels of initial roughness and two slope gradients. Surface microtopography was digitised by a laser scanner before and after each rainfall event. Soil roughness was analysed by the variogram method and its role in runoff triggering was evaluated using a numerical model that gradually fills depressions with a conditioned-walker method. Experimental variograms showed a gradual lowering of semivariances in a homothetic way after each additional rainfall, indicating that all roughness scales are affected similarly. All variograms showed a distinct topographic correlation length that can be related to depressional storage capacity. The linear relationship between these two variables also has a threshold roughness term below which the storage capacity tends to zero. Analyses of the runoff triggering showed that a small modification of micro-topographic structure had a major effect on runoff initiation. Even if the storage capacity is an

* Corresponding author. Presently at: National Soil Erosion Research Laboratory, Purdue University, Building SOIL, West Lafayette, IN 47907-1196, USA. Fax: +1-765-494-5948.

E-mail addresses: darboux@ecn.purdue.edu (F. Darboux), Phillippe.Davy@univ-rennes1.fr (Ph. Davy), cgascuel@roazhon.inra.fr (C. Gascuel-Odoux), chihua@ecn.purdue.edu (C. Huang).

[1] Fax: +33-2-99-28-60-88.

[2] Fax: +33-2-99-28-54-30.

[3] Fax: +1-765-494-5948.

PII: S0341-8162(01)00162-X

important parameter of the runoff characteristics, large differences are observed between the initial stages of each experiment and final stages. We attributed these differences to the creation of preferential connections between topography depressions due to the material redistribution. Since the variogram analysis may not be sensitive toward the development of preferential flow path in a local scale, additional methodologies, such as the conditioned-walker analysis used in this study, need to be incorporated in quantifying the role of surface microtopography on the dynamics of runoff generation.

Keywords: Microtopography; Roughness; Variogram; Storage capacity; Runoff; Connectivity

1. Introduction

Roughness is one of the major parameters controlling overland flow. The overall roughness effects depend on the scales of the processes involved. For mm to cm scales, soil roughness reduces flow velocity and the roughness effect is usually incorporated in a friction term such as Darcy–Weisbach's, Manning's or Chezy's coefficients (Baird et al., 1992; Grayson and Moore, 1992; Scoging et al., 1992). At the decimetre scale, surface clods, ridges, mounds and depressions define the roughness properties. Since water storage in depressions delays overland flow triggering, quantification of storage capacity (i.e., total volume of depressions) has been a subject of numerous researches (Langford and Turner, 1972; Mitchell and Jones, 1976; Gayle and Skaggs, 1978; Huang and Bradford, 1990; Mohamoud et al., 1990). When length scales exceed several decimetres, roughness effects become significant for the flow path.

Runoff generation is a spatially distributed process where surface morphology, in both the macro and micro scales, controls the surface flow routing. At the beginning of a rainfall, water infiltrates. If rainfall intensity exceeds infiltration rate, free water remains on the surface and partly fills depressions. In this stage, runoff amount is limited because the water cannot reach the outflow boundary. If rain persists with an intensity higher than the infiltration rate, puddles progressively overflow and either feed adjacent depressions or connect to the outflow boundary, thus initiating runoff. With additional rainwater, more and more depressions are connected and a network of flow paths is eventually formed. For a defined rainfall intensity–infiltration rate ratio, the flux at the outflow is directly related to the drainage area connected to the outflow boundary. This drainage area is a geometrical notion that depends on both the topography and the quantity of water stored on the surface. Describing further runoff generation is complicated by modifications in soil surface conditions and by the numerous processes among which are erosion and sedimentation in interrill areas.

Surface routing of water in interrill areas has not been extensively studied because the difficulty of acquiring data with small-scale resolution was impractical over sufficiently large surface areas. Moore and Larson (1979) showed that flow paths affect puddle-filling and runoff-triggering. While it was commonly assumed that runoff occurred only after depression storage was satisfied, Moore and Larson (1979) showed that some runoff occurred concurrently with depression filling. Later, using digital elevation models (DEMs) with 15-cm × 1.3-cm resolution for an area of 0.9 m × 1.5 m, Onstad

(1984) showed that the rain amount needed to fill all depressions was greater than the storage capacity (i.e., the mean depression volume per area unit). He confirmed that a certain amount of water contributes to the runoff while depressions are still filling. Because overland flow begins before the complete filling of depressions, the storage capacity is not a good predictor for overland flow genesis. Using 2.6-m × 1.2-m DEMs with 2.5-cm grid size, Sneddon and Chapman (1989) mapped depressions, their connections and drained areas. It appeared that the outflow of a depression did not only depend on its volume, but also on its drained surface area. As shown by Moore and Larson (1979), the increase of runoff coefficient is not continuous and can even reach transient plateaux, indicating that the growth of the area contributing to runoff is often discontinuous. Indeed, the main process is based on the outflow of individually filled depressions, each of them being characterised by an outflow threshold. The relationship between runoff and added water must thus reflect the nature of this discontinuous evolution.

Recently, Helming et al. (1998a,b) performed network geometry analysis on surfaces after simulated rainfall. Their analysis, using techniques developed to characterise river networks, was carried out on 2.8-m × 0.6-m DEMs. These authors examined changes in network properties for eroding surfaces at all-connected states assuming that depressions were completely filled before analyses. They showed that flow paths undergo a decrease in sinuosity and gradient and suggested that the flow network structure evolves into a "self-organised" configuration where overall geometry of flow paths is similar to those developed river networks (fractal dimension, Horton's ratios).

This study is designed to quantify the roughness effects on overland flow genesis with a specific focus on relationships between roughness modifications and the development of water flow network in interrill areas. Changes in surface microtopography after a sequence of rainfall events were quantified utilising a laser scanner. A conditioned-walker model was used to study the process of depression filling and the triggering of runoff. This study is expected to enhance understanding of soil roughness effects on the dynamics of surface runoff generation.

2. Materials and methods

2.1. Experimental procedure

2.1.1. Soil and soil box design

Experiments were carried out at the National Soil Erosion Research Laboratory, West Lafayette, IN, US. The soil was a Glynwood clay loam (fine, illitic, mesic Aquic Hapludalf with 22% sand, 49% silt and 29% clay) with a subangular-blocky structure, collected from Blackford County, IN. A wooden box of 2.4×2.4 m^2 was used in the rainfall simulation study. The box was filled with a 5-cm layer of pea gravel at the bottom and a 7-cm-thick soil layer on top and separated from the gravel by a piece of porous landscape fabric; some space was allowed between the bottom boards. The gravel bed combined with the soil bed thinness was designed to allow free drainage and so to limit the formation of a perched water table.

2.1.2. Rainfall simulators

The rainfall simulators used in this study were similar to those described by Foster et al. (1979). In this type of simulator, rainfall is applied by oscillating nozzles. The flow is also periodically deflected from continuously flowing nozzles. Rainfall intensity is controlled by controlling the frequency at which nozzles pass between their deflectors. Each simulator trough had three Veejet nozzles (Part No. 80100, Spraying Systems, Wheaton, IL) spaced 1.1 m apart. Nozzle pressure was kept at 42 kPa. For this pressure, the mean drop-size is close to 2.2 mm (Meyer and Mac Cune, 1958). Two rainfall simulator troughs, supplied with de-ionised water, were mounted 2.4 m above the soil box and spaced 1.4 m apart. Rainfall intensity was kept equal to 24 mm h^{-1} (± 4 mm h^{-1}) though a slightly lower intensity was observed at the upper and lower portions of the soil box.

2.1.3. Experiments

Two levels of isotropic roughness were specified for the test. A low roughness was created just by keeping elevation variations due to clods. A high roughness was created by hand in order to generate a patterned mound and depression microtopography. In each case, two slopes were used, i.e., 2% and 5%. Hence, four experiments were carried out with the following initial conditions:

1. Low roughness and 2% slope (LR-2%).
2. Low roughness and 5% slope (LR-5%).
3. High roughness and 2% slope (HR-2%).
4. High roughness and 5% slope (HR-5%).

For each of the four experiments, a succession of four rain events was applied. The first two rain events were of 30-min duration. Because roughness tends to evolve more slowly with cumulative rainfall, the third and the fourth events were of 60-min duration. Rainfall was applied once a day. Between rainfalls, soil water was allowed to drain freely and the surface was not covered to allow roughness measurements. After each experiment, two fans were used to dry the surface. During the drying period, the soil was manually turned several times in the box to accelerate drying and to recreate a cloddy structure. It also insured homogenous drying and avoided layering in the soil bed. During soil box preparation, clods larger than 5 cm in diameter were broken up by hand. After each experiment, additional fresh soil was added to compensate for losses.

2.1.4. Microrelief measurements

Microrelief measurements were performed using a 3-m $\times$ 1-m laser scanner (Flanagan et al., 1995) modified from the original design of Huang and Bradford (1990). The laser optics have an elevation resolution of approximately 0.02 mm. For this study, surface elevation was digitised for both horizontal directions in 1-mm grids. To obtain the elevation measurement of the entire box surface, three adjacent scans were performed, each one covering an area of 2.4 m $\times$ 0.8 m. The scanned surfaces were identified with

pins located at their corners. These pins enabled an accurate positioning of laser scanner. This 'benchmarking' was necessary to reconstruct the DEM of the whole soil box by joining the three successively measured DEMs. Missing points caused by shadow effects were linearly interpolated.

Microtopography was measured before the first and after each of the rainfall events. In each experiment, five 2.4-m × 2.4-m DEMs were acquired and identified as "Rain 0" before any rainfall application, "Rain 1" after the first rainfall, etc. In the following discussion, DEMs are identified by the initial roughness level and the soil box slope, i.e., LR-2%, LR-5%, HR-2% and HR-5% and the rainfall event.

2.2. Microrelief analysis

2.2.1. Variogram

A variogram permits the characterisation of spatial correlation (Davis, 1973). This technique has been applied to quantify soil roughness (Linden and Van Doren, 1986; Huang and Bradford, 1992; Huang, 1998). A variogram is defined as:

$$\gamma(l) = \frac{1}{2N}\sum_{x}\left[z(x) - z(x+l)\right]^2 \quad (1)$$

where γ is the semivariance, l is the lag distance between points, $z(x)$ is the elevation at the location x, and N is the number of pairs considered. It gives a relationship between a variance term γ based on elevation difference and the separation length l.

To remove general-slope effects, the elevation $z(x)$ is taken as the distance from the soil surface to the mean plane. Computations for each DEM were performed using the 1-mm resolution grid. Calculations were done for all directions and averaged for each lag distance.

2.2.2. Connectivity development analysis

To produce a spatial analysis related to overland flow process, a gradual puddle-filling model was used. While a variogram can only characterise surface correlation, this process-oriented model directly treats with surface properties significant for water flow, such as depression volumes and flow-path connectivity. The above model, used as a descriptor of surface properties, simulates the rainfall filling of depressions by assuming that: (1) water is randomly distributed over the entire surface; (2) water moves to the lowest point; and (3) water is stored in depressions. This gradual puddle-filling model is based on the conditioned-walker method (Chase, 1992; Favis-Mortlock, 1998) and treats the displacement and trapping of successive individual water elements. The walker is launched at a randomly selected location with a finite amount of water and moves on an evolving surface grid, defined either by the soil surface or by the top surface of the previously deposited water. Its direction of movement is defined by using a maximum slope criterion considering a four-neighbour scheme. If the walker is trapped in a local minimum, it tries to fill it. If the carried amount of water is less than the available volume of the local minimum, the walker deposits all its water and disappears. If the

amount of water is greater than the volume of the local minimum, the walker fills the depression and continues to move with the remaining water using the same maximum slope criterion. In such a way, successive walkers gradually fill depressions.

To simulate a system with a geometry identical to rainfall experiments, the same boundary conditions were used. Because of computer limitations, the DEMs were resampled at 5-mm grid resolution by keeping one point in five for each row and column. Water inflow was computed as the sum of walker volumes added on the surface, water outflow as the sum of the walker volumes reaching the free boundary. The runoff coefficient is the ratio between outflow and inflow volumes over the step considered. Storage capacity is the sum of puddle volumes and is equal to the total rain inflow minus the total runoff outflow when depression filling is completed.

3. Results

3.1. Surface morphology and storage capacity

In the experiments, overland flow was not uniformly distributed on the surface because local heterogeneities in flow depth were caused by the roughness of the surface. Nevertheless, overland flow could be considered as sheetflow. No rill appeared during any experiments and only limited incisions were observed at depression outlets.

All the variograms showed a similar two-straight line trend in a log–log diagram (Fig. 1), with a steep slope at short lag distances, and a gentle slope for lag distances greater than several centimetres. Each log–log straight line scale regime may be modelled by a power law (Fig. 1(a)). The steep slope represents the existence of a correlation at short lag distance. For large lag distance, almost no correlation persists. The transition between these two regimes defines the correlation length of the surface, usually referred as the range (Davis, 1973) and represents the maximum lag distance at which correlation is observed. The slopes of the log–log variograms were almost identical for all experiments at every stage. For each experiment, from rain to rain, the log-semivariance values decreased uniformly regardless of the lag distance but neither the range nor slopes were significantly modified. For the two low-roughness experiments (LR-2% and LR-5%), semivariances were almost identical before the first rain, i.e., after being shaped by the operator (Fig. 1(a),(b)). After successive rainfalls, variograms still remained similar. For high-roughness experiments, initial variograms showed slight differences with greater dm–m scale semivariance for HR-2% than for HR-5% (Fig. 1(c),(d)). This observation indicates the difficulty of obtaining similar initial roughness conditions during surface preparation. This difference persisted throughout the rainfall sequence.

Storage capacities decreased with successive rainfalls (Fig. 2(a)), as expected, since erosion and sedimentation in interrill areas usually tend to decrease the roughness amplitude. In interrill areas, Onstad (1984) demonstrated that the storage capacity was positively related to the roughness, and negatively related to the slope. To compare the different surfaces, we calculated a characteristic roughness as the intersection between the two-scale regimes of the variogram (Fig. 1(a)). The square root of the corresponding

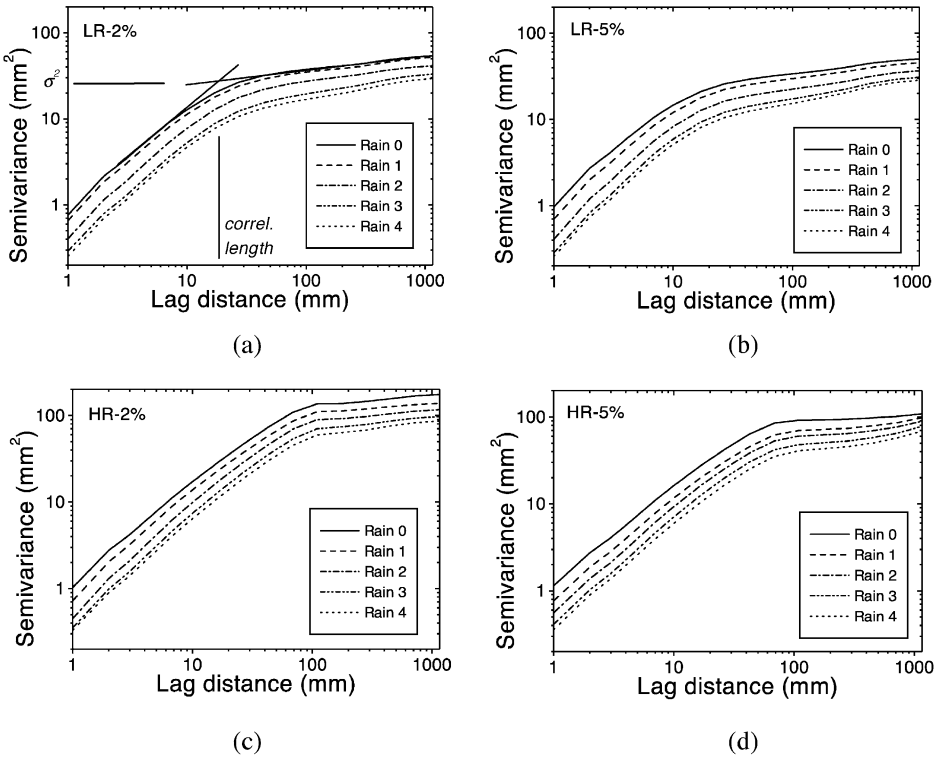

Fig. 1. Variograms computed from the surface DEMs after slope removal for treatments: (a) LR-2% (low roughness—2% slope); straight lines see text; (b) LR-5%; (c) HR-2% (high roughness); (d) HR-5%.

semivariance is expressed in length unit and is the standard deviation of altitudes for points separated by the correlation length. The horizontal length scale of this transition is representative of the average size of the depressions which store the surface water.

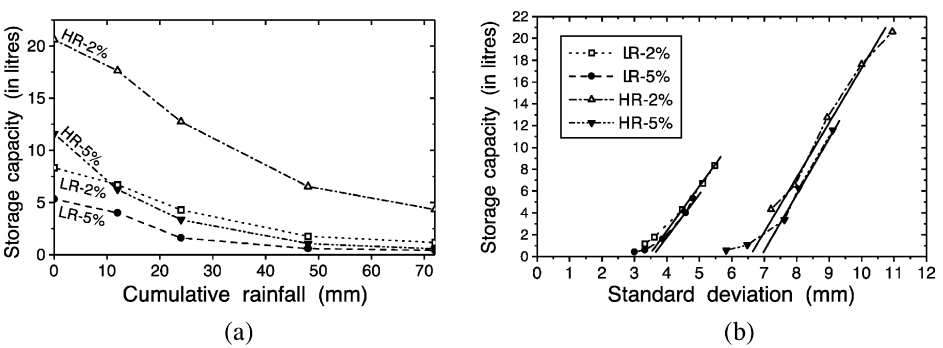

Fig. 2. Evolution of surface storage capacity with successive rainfalls for the four experiments as functions of (a) rainfall event; and (b) standard deviation σ.

Increasing the initial roughness causes an increase in the storage capacity (Fig. 2(b)). A slope effect also exists, since the storage capacity of 5% slope experiments is systematically smaller than the one for 2% experiments of a given roughness.

From the experimental data, we found a general linear trend between the characteristic roughness σ and the storage capacity s:

$$s = A(\sigma - \sigma_0) \quad (2)$$

with A close to 4.10^6 mm^2, if s is expressed in mm^3, and σ and σ_0 in mm. The existence of a threshold σ_0 denotes that rough surfaces can have a nil storage capacity and means that only part of the roughness measured as the standard deviation σ contributes to surface storage. If σ_0 accounts for the roughness that does not contribute to surface storage, $\sigma - \sigma_0$ represents the roughness efficient for storage capacity.

The proportionality coefficient A is a characteristic area of 4 m^2, which is representative of the experimental surface-storing water. A simple interpretation of Eq. (2) is that the storage capacity s represents the volume of depressions having an average depth $\sigma - \sigma_0$ covering a surface A.

The relationship in Eq. (2) holds for the first steps of the surface evolution, when σ is larger than σ_0. For roughness close to, and smaller than σ_0, the storage capacity tends slowly to the zero value while the roughness remains noticeable. The complete relationship between s and σ is a typical threshold curve, in which Eq. (2) only represents the limit for large roughness.

Similar threshold roughness σ_0 were found for the two "HR" experiments (7 mm) and for the two "LR" ones (3.5 mm) (Fig. 2(b)). Even if no replication was performed, it suggests that the σ_0 value depends more on initial roughness than on general slope. The validity of these findings should be investigated by further experiments.

3.2. Depression-filling simulations

The depression-filling model gives some indications about the dynamics of runoff. It helps to show the effect of water storage in depressions on runoff triggering without considering interaction with infiltration. Water is progressively added on the surface until all the depressions were filled. The calculations were made by considering increments of added water, and the runoff coefficient was calculated between two increments. As stated by Onstad (1984), the calculated curves can show irregular shapes with transient plateaux due to the finite amount of water needed to allow a depression to outflow. For the initial stages of the experiments (Fig. 3, solid curves), the relationship between runoff coefficient and added water is sigmoidal with an inflexion point corresponding to a critical value of the total amount of added water. Below and above this critical value, the runoff coefficient increases slightly while the main variations are found around this critical point. For a large volume of added water, the entire system is connected to the free boundary. Any additional added water outflows and the runoff coefficient equals one. As a consequence, the storage capacity is calculated as the difference between the total volume of added water and the total volume of runoff.

With the subsequent rainfall events, the critical water volume required to trigger runoff decreases. The initial plateau can even disappear (see, for instance, experiment

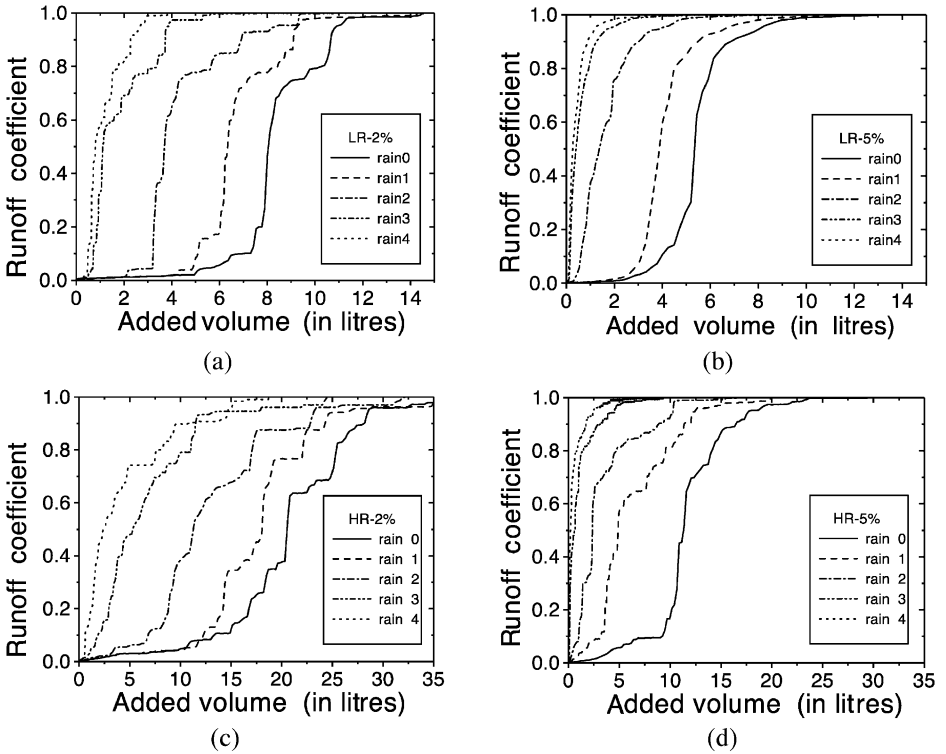

Fig. 3. Runoff coefficient calculated from conditioned-walker model as function of added water for treatments: (a) LR-2% (b) LR-5%; (c) HR-2% (d) HR-5%.

HR-5%, Rains 3 and 4), meaning that a significant runoff can exist for small volumes of added water. The all-connected state (runoff coefficient equal to one) is also reached with a smaller added volume.

Potentially, the dynamics of overland flow triggering may depend on storage capacity and puddle connectivity. Therefore, the real effect of connection development on overland flow genesis can be studied only when considering surfaces with identical storage capacity. We have thus normalised the added volume in the depression-filling model by the storage capacity to highlight the connectivity modification induced by the erosion and sedimentation processes (Fig. 4).

Because the volume of the depressions depends on the particular surface morphology, each surface has its own storage capacity. Thus, each curve was normalised to the storage capacity of the corresponding surface. Because of the renormalisation, a value of one on the horizontal axis means that the added volume is equal to the storage capacity of the surface. For the four experiments, similar evolutions are observed. The LR-5% experiment is probably the clearer example because of the smoothness of the curves. This particularity could be a combined effect of steep slope and low roughness. Solid curves (initial surfaces, Rain 0) have a symmetric shape with an inflexion point for

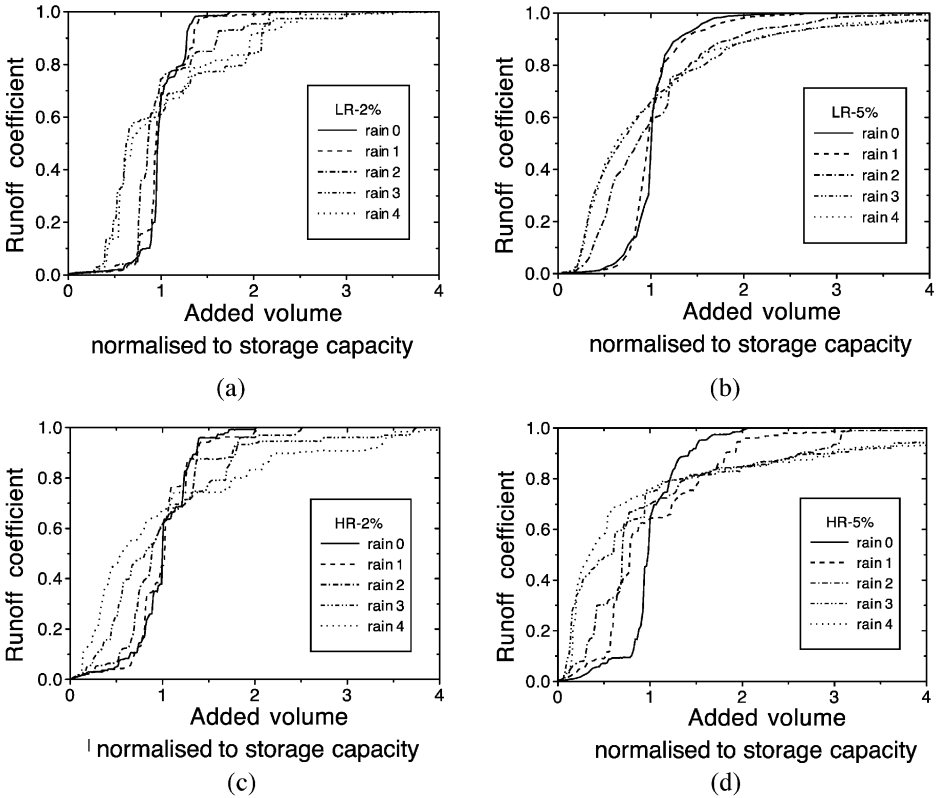

Fig. 4. Runoff coefficient as function of added water normalised to its storage capacity for treatments: (a) LR-2% (b) LR-5%; (c) HR-2% (d) HR-5%.

which the total added volume exactly equals the storage capacity. For a value of approximately twice the storage capacity, almost all the depressions contribute to the runoff flux and the system is said to be in a connected state. The second stage (Rain 1) remains similar, while strong variations are observed at least for the two last stages (Rains 3 and 4). For these later stages, the runoff coefficients reach greater values with much smaller amounts of normalised added rainwater; but the increase in runoff is not as sharp as in the first two stages. The all-connected state is reached for volumes noticeably greater than two. This contrasting evolution may be explained by connectivity properties as illustrated in Fig. 5 for experiment LR-5%. The white part of the figure represents the surface contributing to the outflow, and illustrates in some way the geometrical organisation of the flow paths. For an added volume equal to half the storage capacity (Fig. 5(a),(c)), the runoff coefficient was almost zero for Rain 1 while the runoff coefficient for Rain 3 was 0.45. For Rain 1, only a narrow strip located near the outflow boundary contributed to the runoff, while a widespread area already exists for Rain 3 with a well-defined fingering organisation. In contrast, when the normalised added volume equals two (Fig. 5(b),(d)), the runoff coefficient was about 0.98 for Rain

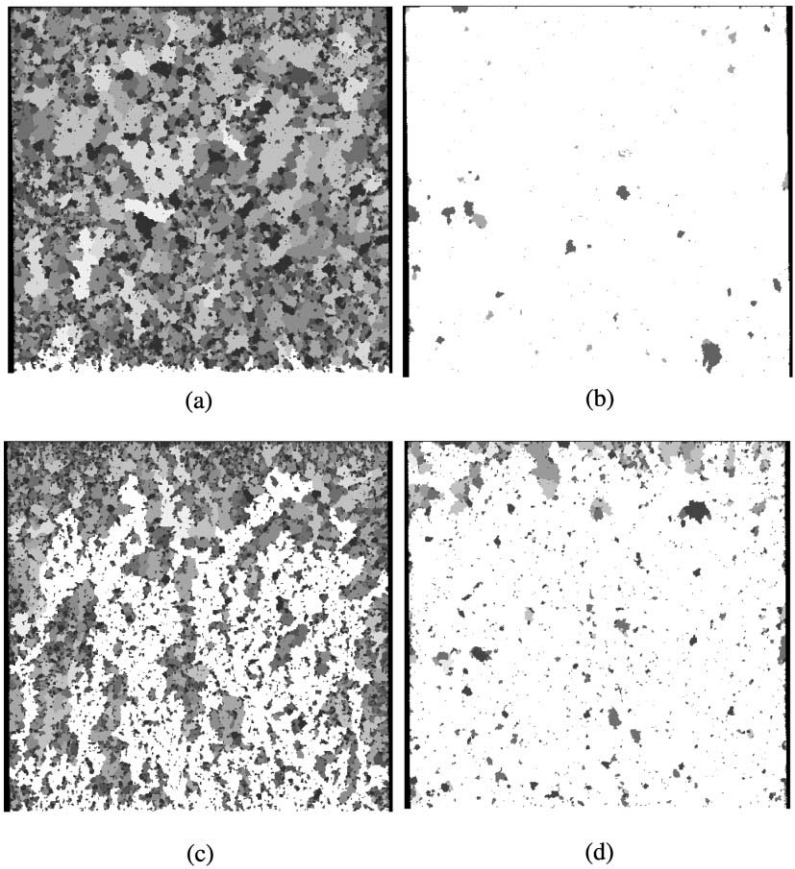

Fig. 5. Spatial distribution of areas (shown in white) contributing to overland flow for the LR-5% experiment. After rain 1: (a) with 0.5 storage volume added; (b) with twice the storage volume added. After rain 3: (c) with 0.5 storage volume added; (d) with twice the storage volume added.

1, and only 0.9 for Rain 3. This difference comes from the numerous unconnected areas remaining for Rain 3, visualised in Fig. 5(d). Though connections among depressions develop simultaneously at first, particle transfer processes lead to differentiation. Because changes in depression volume and drained areas allow some areas to connect more easily than others, connectivity properties become heterogeneous and so the runoff curves lose symmetry.

4. Discussion and conclusion

These experiments demonstrated strong differences between the smooth evolution of the variograms, and the contrasted evolution of the storage capacity and runoff characteristics as calculated with the depression-filling model. A variogram quantifies the

global organisation of the topography. In our experiments, they show a characteristic correlation length in the range of 20–100 mm, depending on the initial roughness. Above this correlation length, the topography is almost uncorrelated. This is quite representative of natural soils which exhibit similar characteristics (Huang and Bradford, 1992). Due to erosion and sedimentation processes, roughness decreases at every scale in a proportion which is almost scale-independent. This continuous decrease of roughness contrasts with the evolution of the storage capacity, and of the runoff characteristics, which both show strong differences between initial and final stages of the surface evolution.

The storage capacity is expected to depend on both the roughness and the experiment slope. By using the roughness index, defined as the standard deviation at the correlation length of the topography, we have obtained a relationship between the storage capacity s and the roughness σ of the form: $s = A(\sigma - \sigma_0)$, where A is about the total area of the system, and σ_0 is a roughness threshold. This relationship holds if σ_0 is larger than σ_0. For smaller σ values, the storage capacity remains close to zero. The value of $\sigma - \sigma_0$ represents the part of the roughness which effectively contributes to the storage capacity. This can be understood by the fact that the volume stored in a depression depends on the lowest altitude of its perimeter. Thus, the effective elevation difference for surface storage is obviously smaller than the roughness calculated from the entire topographic data set. The most surprising result is the existence of a threshold roughness σ_0, which depends only on the initial soil surface shape. The determination of the threshold roughness σ_0 becomes a key-point for further studies. A main difference between low-roughness experiments, for which σ_0 is about 3 mm, and high-roughness experiments, for which σ_0 is about 7 mm, is the correlation length measured by the variograms. Correlation length is about 15 mm in the former experiments, and about 70 mm in the latter ones. A relationship could exist between correlation length and threshold roughness. This relationship could allow to a measure of threshold roughness using a variogram. These preliminary findings need further investigation.

However, the storage capacity alone is insufficient to characterise the triggering of the runoff. The depression-filling simulations show that erosion and sedimentation induce strong differences in the runoff characteristics. For the very first stages of each experiment, the runoff is triggered for a volume of water equal to the storage capacity. The runoff coefficient passes from almost zero to one with a small amount of added water, meaning that most of depressions connect at once to the outflow boundary, at the very point at which added volume equal storage capacity. This behaviour is probably caused by the initial homogeneity of depression properties, i.e., similar sizes and the absence of preferential connections. For the later stages, the runoff is triggered by added water volumes much smaller than the storage capacity. Paradoxically, the amount of water needed to in-fill all the depressions is significantly larger than the storage capacity (more than five times). Water that runs off early will not contribute to depression filling, explaining why the connection of the entire surface to the outflow boundary is difficult to achieve.

By these later stages, the microtopography has been modified by erosion and sedimentation processes which create connected paths between puddles. An example of an eroded topography is given in Fig. 6(b) and compared with an initial stage (Fig. 6(a)).

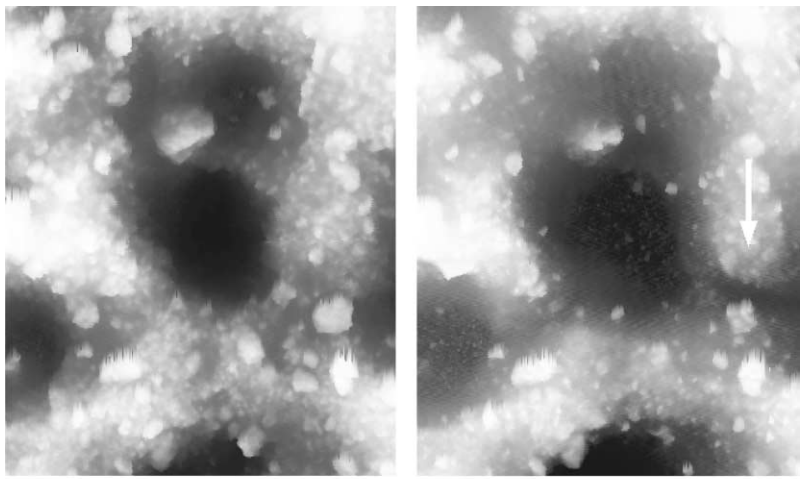

(a) (b)

Fig. 6. Changes in morphology in surface depressions for a 40-cm wide area for the HR-2% treatment after (a) Rain 1; and (b) Rain 4. Elevations increase from black to white.

The shape of the topography is not strongly modified except a local channel incised at the outlet of the puddle (see arrow in Fig. 6(b)). These small modifications of the topography cannot be captured by a variogram analysis, but their effect on the runoff process is very important since they connect puddles together and, eventually, to the outflow boundary. This connectivity gives specific properties to the surface connected to the outflow boundary, as illustrated in Fig. 5. Initially, the connected surface spreads across almost the whole box, connecting points very far from the outflow boundary. In later stages, this connected surface is heterogeneous, has a fingering organisation, and thus represents only a fraction of the total surface (45% in Fig. 5(c). In contrast, the remaining surface is more difficult to connect, probably because these zones are not strongly affected by erosion and sedimentation processes. This evolution is consistent with the development of a drainage network suggested by Helming et al. (1998b). Because this previous study considered only completely developed networks, it ignored the role of areas which do not connect easily, a process important for describing runoff characteristics.

A consequence of the present study is that the variogram analysis, which measures average properties of the surface topography, cannot be used to deduce the dynamics of runoff generation. Two problems immediately arise. First, the storage capacity is related to an effective roughness different from the one that can be measured from the variogram. The relationship given in Eq. (2) is one way to overcome this limitation.

Another difficulty arises because runoff characteristics are partly controlled by some details of the surface morphology. In fact, erosion and sedimentation processes are not uniformly distributed and small incisions at puddle outflows have dramatic consequences on the runoff triggering. These important structures of the surface morphology

are not quantified by usual topography analysis, especially because the general shape of depressions are preserved (Fig. 6). Any suitable procedure for determining runoff characteristics must account for details of depression morphology.

Acknowledgements

The authors sincerely thank Rorke Bryan and an anonymous reviewer for helpful comments on the first version of this paper.

References

Baird, A.J., Thornes, J.B., Watts, G.P., 1992. Extending overland-flow models to problems of slope evolution and the representation of complex slope-surface topographies. In: Parsons, A.J., Abrahams, A.D. (Eds.), Overland Flow. Hydraulics and Erosion Mechanisms. Univ. College London Press, London, pp. 199–233.

Chase, C.G., 1992. Fluvial landsculpting and the fractal dimension of topography. Geomorphology 5, 39–57.

Davis, J.C., 1973. Statistics and Data Analysis in Geology. Wiley, New York.

Favis-Mortlock, D., 1998. A self-organizing dynamic systems approach to the simulation of rill initiation and development on hillslopes. Comput. Geosci. 24 (4), 353–372.

Flanagan, D.C., Huang, C., Norton, L.D., Parker, S.C., 1995. Laser scanner for erosion plot measurements. Trans. ASAE 38 (3), 703–710.

Foster, G.R., Eppert, F.P., Meyer, L.D., 1979. A programmable rainfall simulator for field plots. Proceedings of Rainfall Simulator Workshop, Tucson, Arizona, USA. United States Department of Agriculture–Science and Education Administration, Agricultural Reviews and Manuals, Sidney, Montana, USA, ARM-W-10, pp. 45–59.

Gayle, G.A., Skaggs, R.W., 1978 Surface storage on bedded cultivated lands. Trans. ASAE 21(1): 101–104, 109.

Grayson, R.B., Moore, I.D., 1992. Effect of land-surface configuration on catchment hydrology. In: Parsons, A.J., Abrahams, A.D. (Eds.), Overland Flow. Hydraulics and Erosion Mechanisms. Univ. College London Press, London, pp. 147–175.

Helming, K., Römkens, M.J.M., Prasad, S.N., 1998a. Surface roughness related processes of runoff and soil loss: a flume study. Soil Sci. Soc. Am. J. 62, 243–250.

Helming, K., Römkens, M.J.M, Prasad, S.N., Sommer, H., 1998b. Erosional development of small scale drainage networks. In: Hertgarten, S., Neugebauer, H.J. (Eds.), Process Modelling and Landform Evolution. Lect. Notes Earth Sci., vol. 78, Springer, Berlin, Germany, pp. 123–146.

Huang, C., 1998. Quantification of soil microtopography and surface roughness. In: Baveye, P., Parlange, J.-Y., Alton Stewart, B. (Eds.), Fractals in Soil Science. CRC Press, Boca Raton, FL, USA, pp. 153–168, Chap. 5.

Huang, C., Bradford, J.M., 1990. Portable laser scanner for measuring soil surface roughness. Soil Sci. Soc. Am. J. 54, 1402–1406.

Huang, C., Bradford, J.M., 1992. Applications of a laser scanner to quantify soil microtopography. Soil Sci. Soc. Am. J. 56, 14–21.

Langford, K.J., Turner, A.K., 1972. Effects of rain and depression storage on overland flow. Trans. Inst. Eng., Aust. CE 14 (2), 137–141.

Linden, D.R., Van Doren Jr., D.M., 1986. Parameters For characterizing tillage-induced soil surface roughness. Soil Sci. Soc. Am. J. 50, 1560–1565.

Meyer, L.D., Mac Cune, D.L., 1958. Rainfall simulator for runoff plots. Agric. Eng. 39 (10), 644–648.

Mitchell, J.K., Jones Jr., B.A., 1976. Micro-relief surface depression storage: analysis of models to describe the depth-storage function. Water Resour. Bull. 12 (6), 1205–1222.

Mohamoud, Y.M., Ewing, L.K., Boast, C.W., 1990. Small plot hydrology—1. Rainfall infiltration and depression storage determination. Trans. ASAE 33 (4), 1121–1131.

Moore, I.D., Larson, C.L., 1979. Estimating micro-relief surface storage from point data. Trans. ASAE 22 (5), 1073–1077.

Onstad, C.A., 1984. Depressional storage on tilled soil surfaces. Trans. ASAE 27 (3), 729–732.

Scoging, H., Parsons, A.J., Abrahams, A.D., 1992. Application of a dynamic overland-flow hydraulic model to a semi-arid hillslope, Walnut Guch, Arizona. In: Parsons, A.J., Abrahams, A.D. (Eds.), Overland Flow. Hydraulics and Erosion Mechanisms. Univ. College London Press, London, pp. 105–145.

Sneddon, J., Chapman, T.G., 1989. Measurement and analysis of depression storage on a hillslope. Hydrol. Processes 3, 1–13.